Regional ocean grid refinement and its effect on simulated atmospheric climate

Regional ocean grid refinement and its effect on simulated atmospheric climate

Jonny Williams[1]*, Erik Behrens[1], Olaf Morgenstern[1], Wolfgang Hayek[1], João Teixeira[2], Vidya Varma[1,3]

[1] National Institute of Water and Atmospheric Research (NIWA), Wellington, New Zealand
[2]Met Office, Fitzroy Road, EX1 3PB, Exeter, United Kingdom
[3]Now at GEOMAR, Düsternbrooker Weg 20, 24105 Kiel, Germany
*Corresponding author: Jonny Williams, jonny.williams@niwa.co.nz

Key words: Climate, Simulation, Validation

ABSTRACT

In this work we analyse the impact of including a regional, high-resolution ocean model on simulated atmospheric climate in a coupled earth system model. The resolution of the regional, nested ocean model is approximately 0.2° compared to the ~1° resolution of the global ocean model within which it is embedded and this work complements previously published work on ocean circulation and marine heatwaves using this setup, referred to as the New Zealand Earth System Model, NZESM. After a brief discussion of the wider model setup, the persistent Southern Ocean warm bias in climate models and the validation data sets used, we show the effects of the altered ocean physics on air temperature, precipitation and evaporation, latent and sensible surface heat balances, westerly winds, the storm track and the effect on total cloud amount. Overall we find that the NZESM provides a better representation of regional atmospheric climate compared to its parent model – UKESM1 – although this improvement is not universal. For example, although the NZESM shows better agreement in surface air temperature within the nested ocean region, there is also some deterioration in the agreement at higher southern latitudes where the seasonal sea ice edge coincides with a transition from negative to positive correlation between air temperature and cloud amount. The lack of additional model tuning in the NZESM after the nested ocean model's inclusion largely accounts for the presence of these improvement-deterioration pairs with respect to observations. The reader is encouraged to read the paper of Behrens et al. (Behrens et al, 2020) before this one since it provides much additional information which will aid understanding. This study aims to provide a high-level reference ontology for how changing one aspect of the ocean physics in a coupled model can impact simulated atmospheric climate.

1. INTRODUCTION

This paper examines the effect on simulated atmospheric climate of altered ocean physics in a coupled Earth System Model by comparing outputs from a control model, UKESM1-0-LL (Sellar et al, 2020) ('UKESM1') and the New Zealand Earth System Model, NZESM (Williams et al, 2016). This work is a companion, description paper to previous oceanographic studies (Behrens et al, 2020, 2022), focusing on multi-year, annual means. The physical oceanography of the NZESM is described in detail in (Behrens et al, 2020) and the only difference to UKESM1 is the inclusion of an embedded high-resolution ocean model in the New Zealand region, which allows the model to simulate ocean eddies rather than parameterising them.

Climate models' representations of Southern Ocean climate are subject to some persistent biases in the literature and a warm bias with respect to observational products is one of the best known. What this means in practice is that,

in general, climate models do not represent the surface temperature of the Southern Ocean and its overlying atmosphere as well as other regions. The interested reader is referred elsewhere for an in-depth historical review of this using data from the last three Intergovernmental Panel on Climate Change Assessment Reports (Beadling et al, 2020). The goal of improving our understanding of the climate of the Southern Ocean and Antarctica – New Zealand's 'Deep South' – is the driving goal of the New Zealand Government's Deep South National Science Challenge, and indeed the NZESM itself (Williams et al, 2016).

Southern Ocean biases in coupled climate models are typically two-fold, manifesting in a persistent surface warm bias of the Southern Ocean (e.g. Yool et al, 2021) and in a large shortwave cloud radiative effect bias in the overlying atmosphere (e.g. Varma et al, 2020). In coupled models these biases are inherently connected in that, for example, an ocean surface that is too warm will also result in an atmospheric radiation bias which in turn will affect cloud formation, and so on. The Southern Ocean biases in the precursor to UKESM1, HadGEM2-ES, – results from which were submitted to the 5th Coupled Model Intercomparison Project (CMIP5) (Taylor et al, 2012) – are discussed in detail elsewhere (Hawcroft et al, 2016). In the results section below, we focus on changes to

1. Air temperature and surface heat flux.
2. The hydrological cycle.
3. Westerly winds and the storm track.

The impact of tropical cyclones on New Zealand and mid-latitudes in general is the subject of a separate indepth study (Williams et al, 2023). The main aim of this work is to act as a standard, relatively brief reference for future work on the atmospheric climate of the NZESM and as such seasonal variability of the discussed variables is deliberately not included so as to strike a balance between maximising the number of meteorological variables shown whilst remaining relevant to the general reader.

2. MODELS AND VALIDATION DATASETS

The atmospheric component of the models used here is the 'Global Atmosphere Model, Version 7.1' – GA7.1 (Walters et al, 2019) – configuration of the Unified Model. It uses a semi-implicit, semi-Lagrangian dynamical core (Wood et al, 2014), the SOCRATES radiation scheme, based on (Edwards et al, 1996), shallow and deep mass-flux-based convection - e.g. (Gregory et al, 1990) - and sub-gridscale boundary layer turbulence e.g. (Brown et al, 2008). The models also simulate explicit tropospheric and stratospheric chemistry (Archibald et al, 2020).

The configuration of the NZESM described here includes a two-way nested, high-resolution ocean model in the New Zealand region whilst keeping all other aspects of the ocean model unchanged. This nesting has been achieved using the Adaptive Grid Refinement In Fortran – AGRIF – method (Debreu et al, 2008) and has improved the nominal ocean grid resolution from 1° to 0.2°, making it 'eddy permitting', rather than small-scale eddies needing to be parameterised (Hewitt et al, 2020). Previous studies using similar ocean model nesting methods have addressed radioactive isotope dispersal (Behrens et al, 2012) and the ocean circulation of the Agulhas current off southern Africa (Biastoch et al, 2008) for example. A 2019 study gives a further example of how this nesting procedure affects model results when a regional nest at five times higher resolution than that one it is embedded within (the same as the NZESM), albeit at a significantly higher base resolution than UKESM1 (Schwarzkopf et al, 2019).

The ocean model used is NEMO version 3.6 (Gurvan et al, 2022), which contains the MEDUSA ocean biogeochemistry simulator version 2.1 (Yool et al, 2013) and is coupled to the sea ice model CICE version 5.1.2 (Hunke et al, 2017; Ridley et al, 2018). In the nested ocean model, the ocean diffusivity and viscosity are different to the global model and the integration time step is reduced from 2,700s to 900s. The AGRIF formulation is described in detail elsewhere (Behrens et al, 2020).

Throughout this work we compare 20-year annual means (1989-2008) of climate model output to observational and reanalysis products of temperature, precipitation and evaporation, heat fluxes, zonal winds and total cloud amount. The models runs are started in 1950 to enable model spin-up to occur and both models start from initial conditions from a UK Met Office simulation (Tang et al, 2019), which was itself run from 1850. We use data from the ERA5 reanalysis (Hersbach et al, 2020), surface heat flux data from the Objectively Analyzed Air–Sea Heat Fluxes data set (Yu et al, 2007) – hereafter 'OA flux' – and cloud cover from the International Satellite Cloud Climatology project, ISCCP (Rossow et al, 2004; Rossow et al, 1999).

3. RESULTS

3.1 Temperature and surface heat balance

3.1.1 1.5m temperature

Figure 1 shows annual mean 1.5m air temperature for UKESM1 and the NZESM compared to the ERA5 reanalysis (Hersbach et al, 2020).

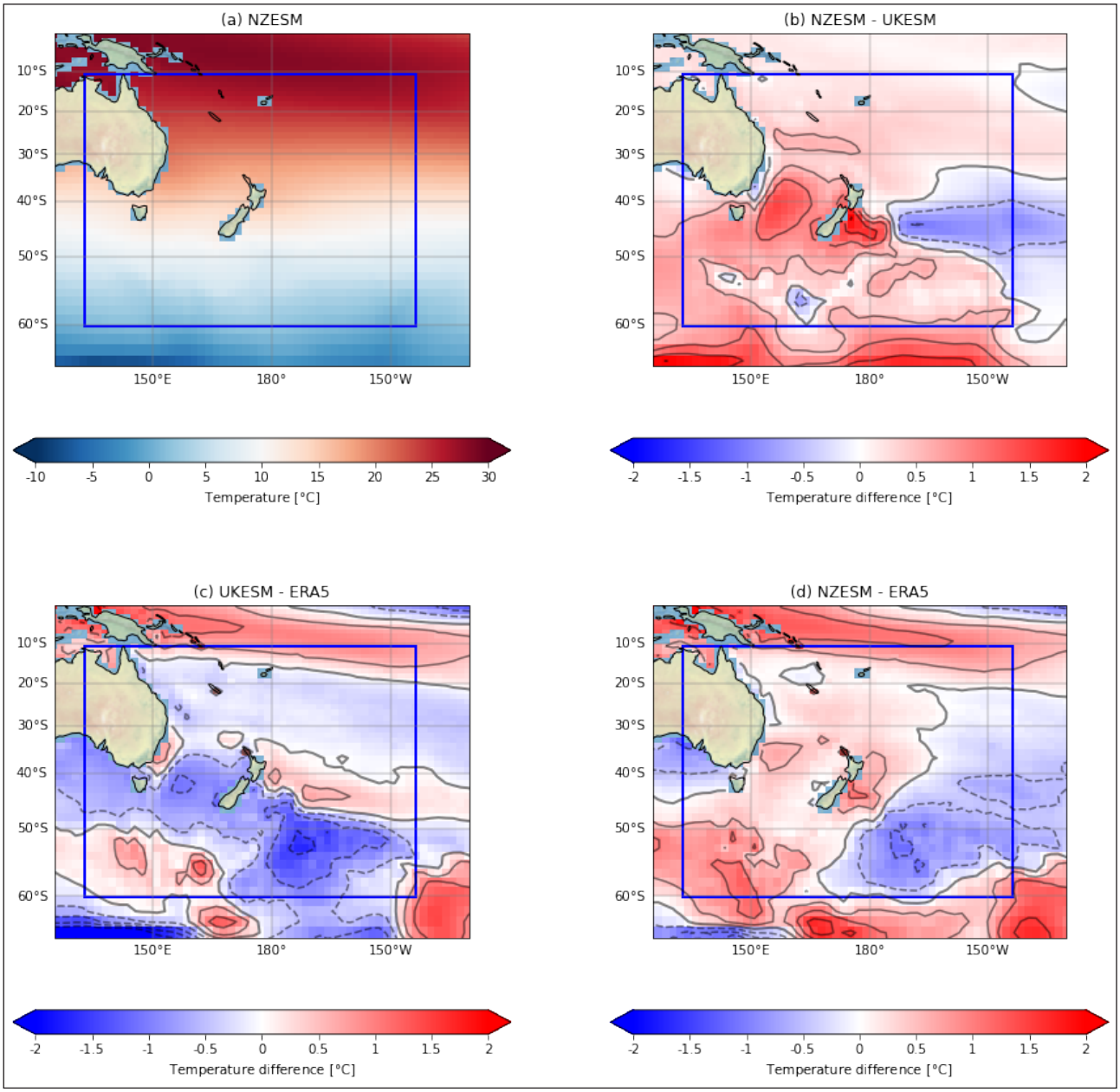

Figure 1: 1.5m annual mean air temperature (°C) for: (a) NZESM (b) NZESM - UKESM; (c) NZESM - ERA5 reanalysis; (d) UKESM - ERA5 reanalysis. All data shows annual means for 1989-2008. The region defined by the blue rectangle denotes the location of the high-resolution nested ocean model, i.e. 'the AGRIF region', after the method used to implement it (Behrens, 2020; Behrens et al, 2020; Debreu et al, 2008). Negative (positive) contours are shown as dashed (solid) lines.

The ocean data in (Behrens et al, 2020) uses the EN4 climatology for sea surface temperature (Good et al, 2013) and therefore this serves as an interesting comparison to a previous analysis of, ostensibly, the same quantity but with a different 'ground truth' data set.

The agreement with the ERA5 reanalysis is improved in the NZESM in some regions (e.g. Tasman Sea, east of New Zealand) and degraded elsewhere (higher latitudes to the south of Australia). The steady state atmosphere results shown in Figure 1 are analogous to the SST data shown in the paper describing the oceanography of this model pair (Behrens, 2013) where detailed information regarding ocean current changes and their effects on surface temperature and salinity, for example, is given.

The warming seen in the NZESM around -60°S in Figure 1(b) is also visible at even higher southern latitudes. This is shown elsewhere (Behrens et al, 2020) and later in this study in relation to the effect of the AGRIF region on the storm track, Figure 12(c) where the NZESM exacerbates the Southern Ocean warm bias already present in UKESM1. This is most notable in the warming of the southern Indian Ocean in the NZESM cf. UKESM1 – Figure 9(a) in the 2020

study detailing the physical oceanography of this model pair (Behrens et al, 2020). These 'far field' changes can be attributed to ocean circulation changes which increase the southward heat flux in the ocean which, over time, bring the surface atmosphere into this new, warmer equilibrium state. This combination of a localised improvement accompanied by an associated deterioration elsewhere is often encountered in climate model development where new physical parameterisations are included without any additional model tuning. The tuning of climate models has its own extensive literature and the interested reader is referred elsewhere (Hourdin et al, 2017; McNeall et al, 2020; Schmidt et al, 2017).

3.1.2 *Temperature as a function of pressure*

Figure 2 shows zonal mean temperature profiles for the region shown in Figure 1.

The tropospheric warming signal in the NZESM is clearly visible in Figure 2(b), as is the accompanying stratospheric cooling, which is thermodynamically required in order to achieve overall energy balance (Pisoft et al, 2021). Due to the warming in the NZESM's low-to-middle-atmosphere, the tropopause is raised by up to ≈130m (Figure 3). Figure 3 shows the tropospheric pressures for the models and the difference between the tropospheric heights.

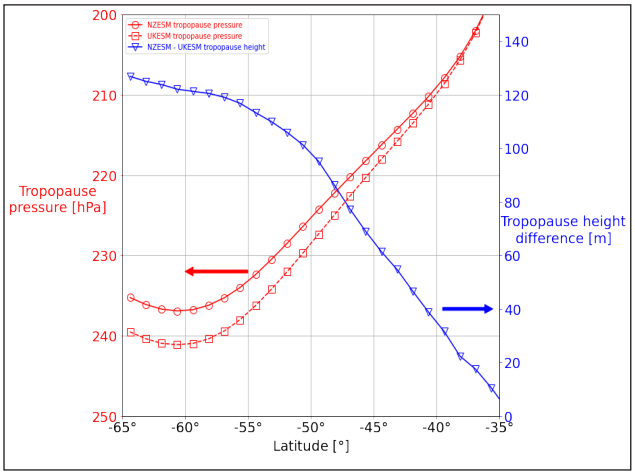

Figure 3: Tropopause pressures in Figure 2 (red) and the tropopause height difference (blue).

Although this is only ~1% of the total height of the tropopause in this region it has been shown that the global warming signal for 20°N – 80°N has been ≈ 50 – 60m per decade for the period 1980-2020 (Meng et al, 2021) and so this response of the lower stratosphere is far from trivial and reflects the importance of coupled modelling in understanding seemingly disparate aspects of the earth system under climate change.

The agreement between the tropospheric temperatures in the NZESM versus the reanalysis data is markedly

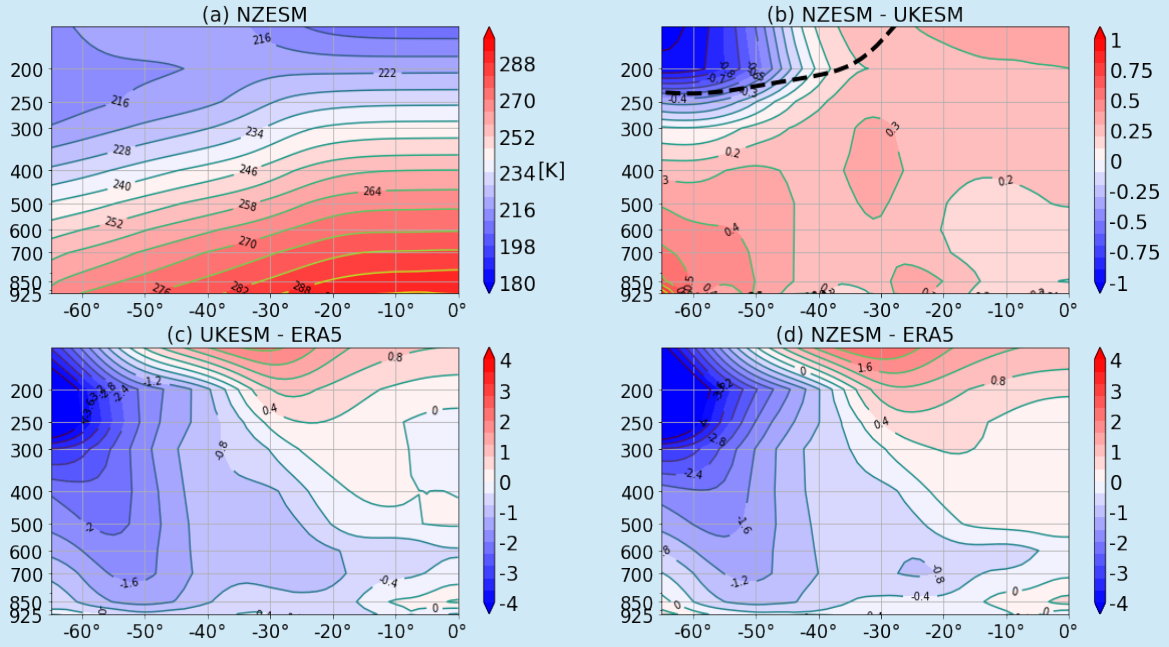

Figure 2: Temperature as a function of pressure: (a) NZESM, (b) NZESM - UKESM (c) NZESM - ERA5 reanalysis, (d) UKESM - ERA5 reanalysis. All data is for 1989-2008 and the thick dashed line in (b) shows the NZESM tropopause in this region.

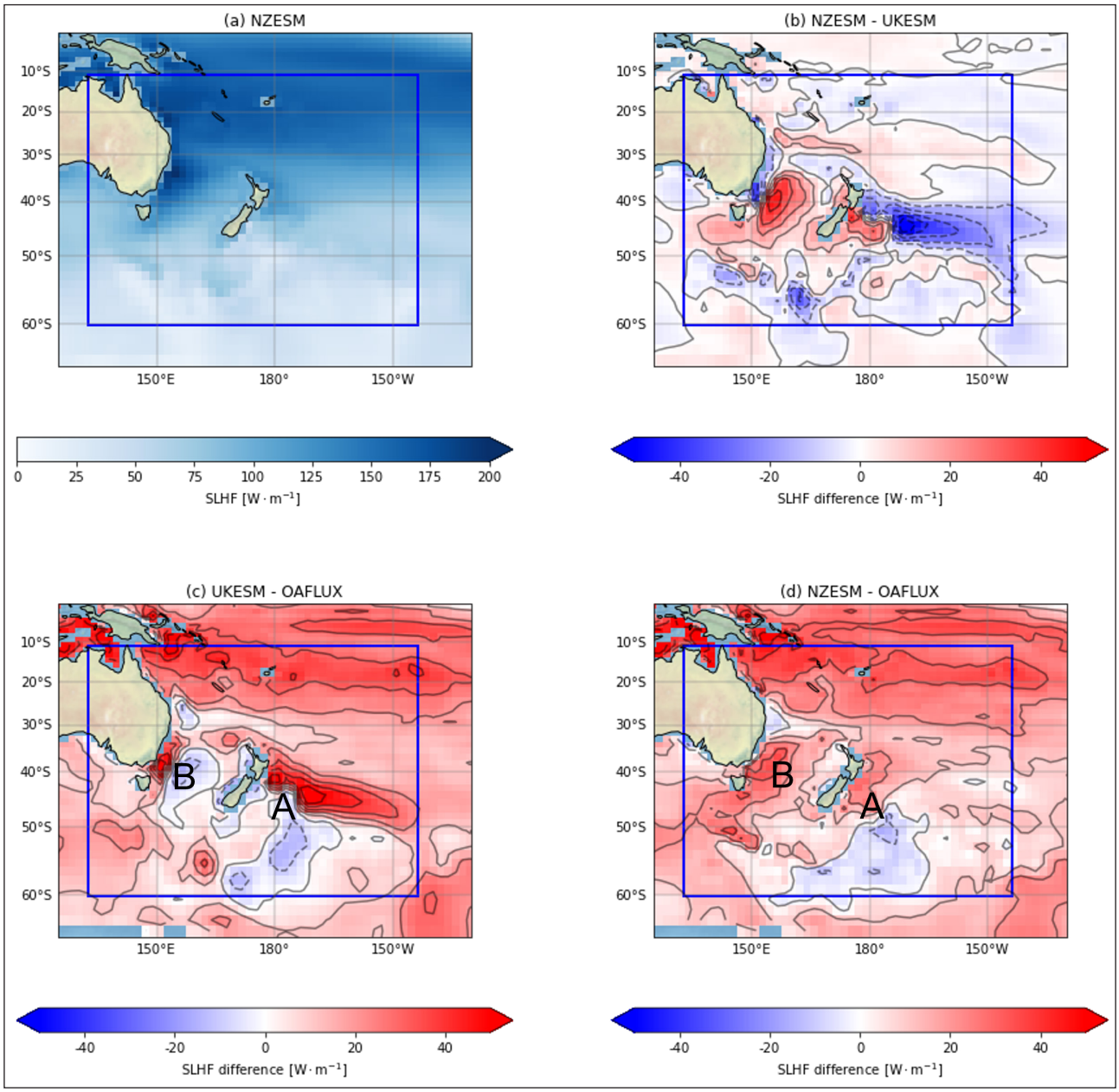

Figure 4: Surface latent heat fluxes (W · m^{-2}) for the models and with respect to the OA flux data set (Yu et al, 2007). (a) NZESM (b) NZESM - UKESM; (c) NZESM - OA flux; (d) UKESM - OA flux.

improved in the mid-to-lower troposphere. There is some deterioration in the agreement in the stratosphere but this is of much smaller extent that the formerly mentioned improvement.

The general warming observed in the NZESM is primarily due to increased southward heat transport by the eddy-permitting ocean, which is discussed in detail elsewhere (Behrens et al, 2020, 2022). This of course not only affects the surface temperature but the structure of the surface heat balance.

3.1.3 Surface heat balance

Figures 4 and 5 show the surface latent and sensible heat fluxes respectively for the models versus the OA flux data set (Yu et al, 2007).

The anomalies' spatial responses in Figures 4 and 5 is - as expected - very similar to temperature response in Figure 1. In both cases, the model-reanalysis data agreement is improved in the NZESM; this is particularly striking in the case of the sensible heating, which shows significantly improved model-reanalysis agreement to the east of New Zealand. The improvement to model-data agreement in this region can be attributed to the decrease in SST in this region in the NZESM, thereby reducing upward heat

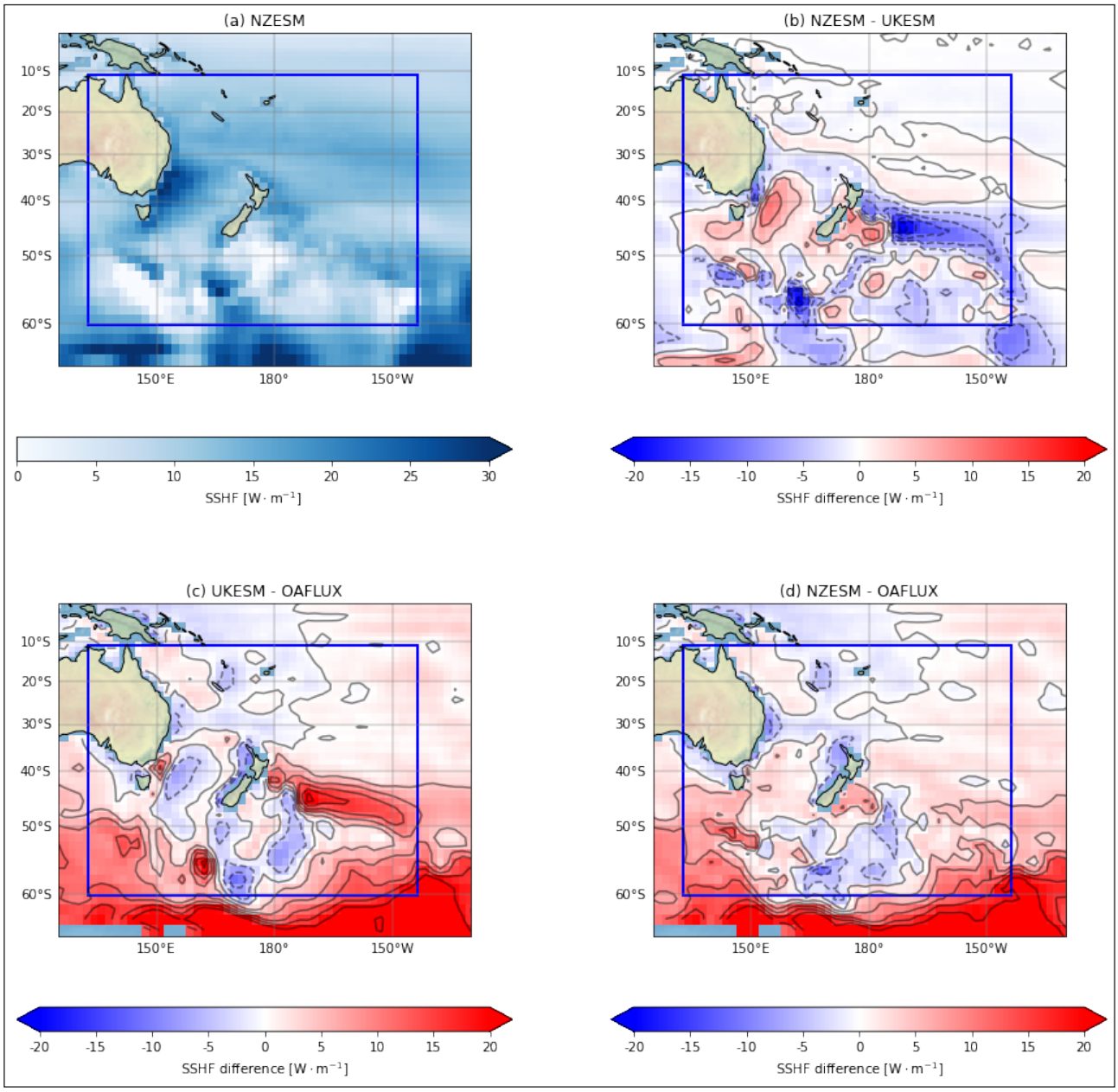

Figure 5: Surface sensible heat fluxes (W · m^{-2}) for (a) NZESM (b) NZESM - UKESM; (c) NZESM - OA flux; (d) UKESM - OA flux.

flux and the positive bias seen in Figure 5(c). The wider relationship between temperature, clouds and radiation is a topic of ongoing research by many authors and represents a 'grand challenge' of coupled climate modelling (Hoem et al, 2022; Hyder et al, 2018; Luo et al, 2023; Varma et al, 2020).

The significant positive sensible heat bias in both models at higher southern latitudes (outside the AGRIF region) is indicative of the warm bias in that region however the agreement within the boundaries of the eddy-permitting ocean is encouraging, illustrating that improved ocean circulation has beneficial effects on atmospheric climate in this coupled framework. In the case of the latent heating there are some areas of improvement – in the region of convergence of the Southland and East Auckland Currents; 'A' in Figure 4(c,d) – and deterioration – Tasman Sea and the south east coast of Australia in particular; 'B' in Figure 4(c,d). That said, there is a clear overall improvement in the model-data agreement in Figure 4.

3.2 Precipitation, evaporation and cloud amount

The hydrological cycle is now considered by examining precipitation, evaporation, total evapotranspiration and total cloud amount. Firstly, Figure 6 shows the annual mean total precipitation fluxes for the models against ERA5

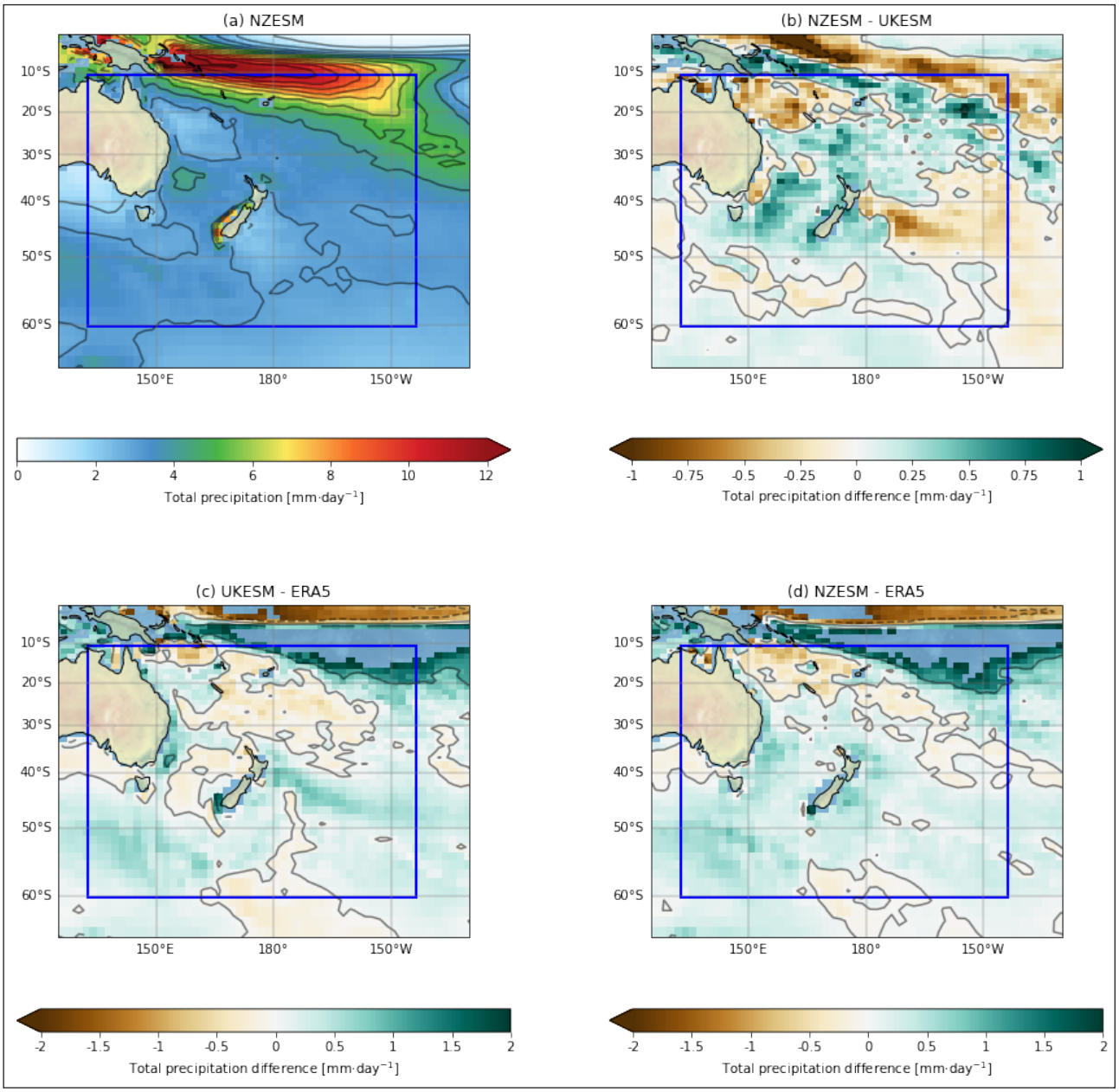

Figure 6: Total precipitation (mm · day^{-1}) for (a) NZESM, (b) NZESM - UKESM, (c) UKESM - ERA5, (d) NZESM - ERA5. Contour levels for levels for all plots are at integer values and for (c) and (d) values over 2mm · day^{-1} are masked to aid visual interpretation.

reanalysis data.

Figure 6(b) shows that the largest changes to the total precipitation come from the South Pacific Convergence Zone – SPCZ – in the northern and eastern portions of the region studied. This region of intense precipitation inclines south-eastwards from the Maritime Continent and is displaced southward in the NZESM cf. UKESM1. This is evidenced by drying in the far northeastern portion and the moistening immediately south thereof in Figure 6(b) and also in the drying signal which occurs in a narrower band in Figure 6(d) with respect to ERA5 cf. Figure 6(c). We also see a general drying to the east and a moistening to the west of New Zealand, which is anti-correlated to the 1.5m temperature changes observed in Figure 1(b) and that the NZESM reduces both wet and dry biases close to New Zealand.

Figures 7 and 8 show sea to air evaporation flux and precipitation minus evaporation *(P - E)* for the model and ERA5 respectively.

Overall, the pattern of changes in the NZESM cf. UKESM1 in the evaporation are of the same sign as the precipitation but larger in magnitude, so $\Delta E > \Delta P$ – compare Figures 6(b) and 7(b). This means that overall changes to surface evapotranspiration – i.e. $\Delta(P-E)$ – are of the opposite

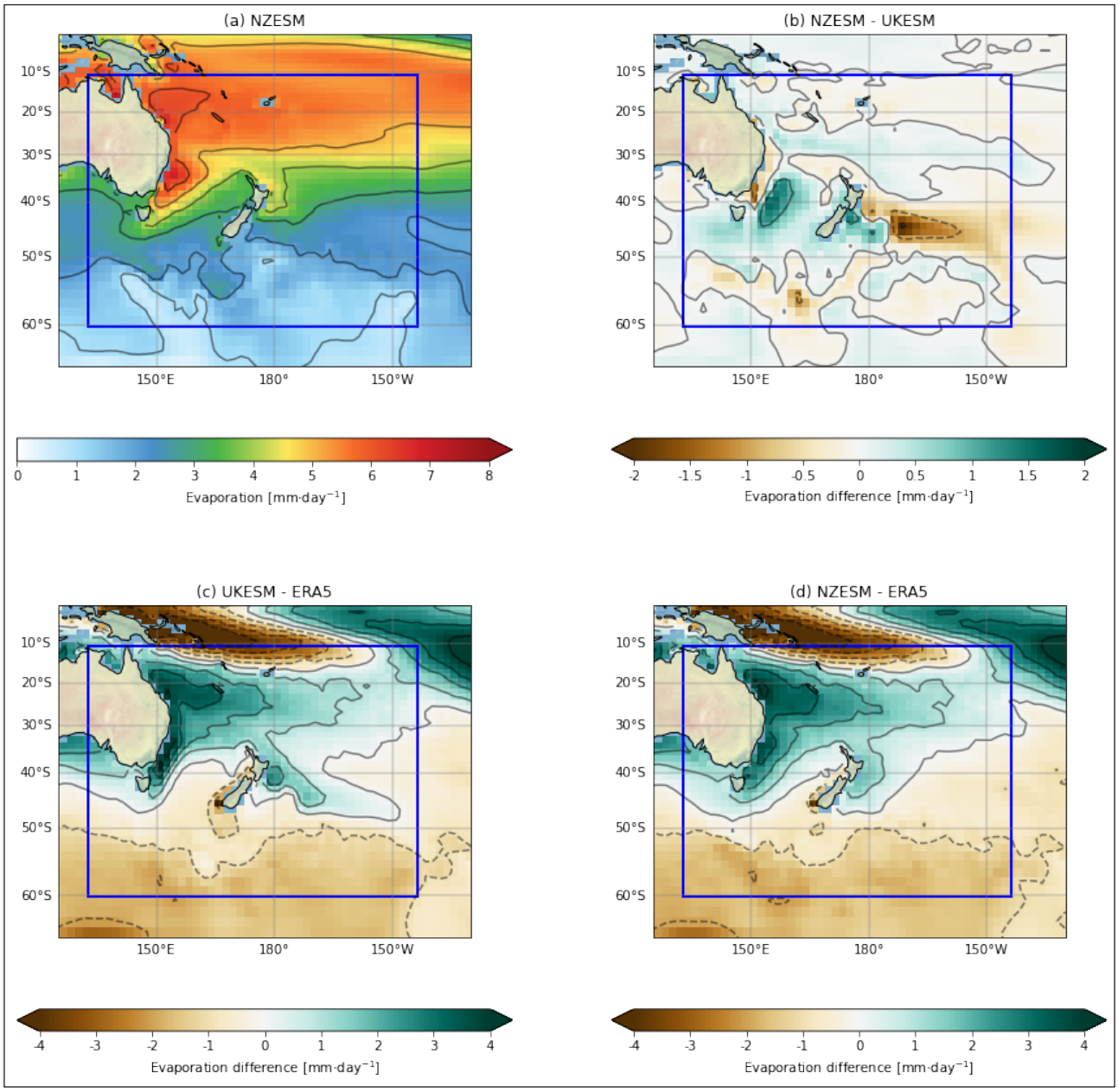

Figure 7: Sea to air evaporation (mm · day⁻¹) for (a) NZESM, (b) NZESM - UKESM, (c) UKESM - ERA5, (d) NZESM - ERA5. Contour levels for levels for all plots are at integer values.

sign to changes in precipitation. Precipitation changes are often considered in isolation in model sensitivity studies and this can have counter-intuitive effects on, for example, surface ocean composition and circulation where regions of increased precipitation could exhibit *increased* salinity and density, in spite of the increased water input from rainfall.

3.2.1 *Cloud amount*

Figure 9 shows the response of the total cloud amount in the models (Bodas-Salcedo et al, 2011) as defined by the International Satellite Cloud Climatology Project, ISCCP (Rossow et al, 1999).

Figure 9(b) shows that there is a general increase in cloud in the NZESM to the east of New Zealand. The reverse seen in the SPCZ and around the Tasman Sea. At mid-latitudes, the sign of this change is anti-correlated with the temperature change – Figure 1(b), Figure 10 below – and in the SPCZ there is a clear relationship between the reduction in total cloud and the amount of precipitation, Figure 6(b). At higher latitudes, the sign of the relationship between increasing temperature and cloud cover is reversed and there is clear increase in total cloud amount in the vicinity of the maximum sea ice extent.

In each ocean grid-box, the prognostic, overlying sea ice

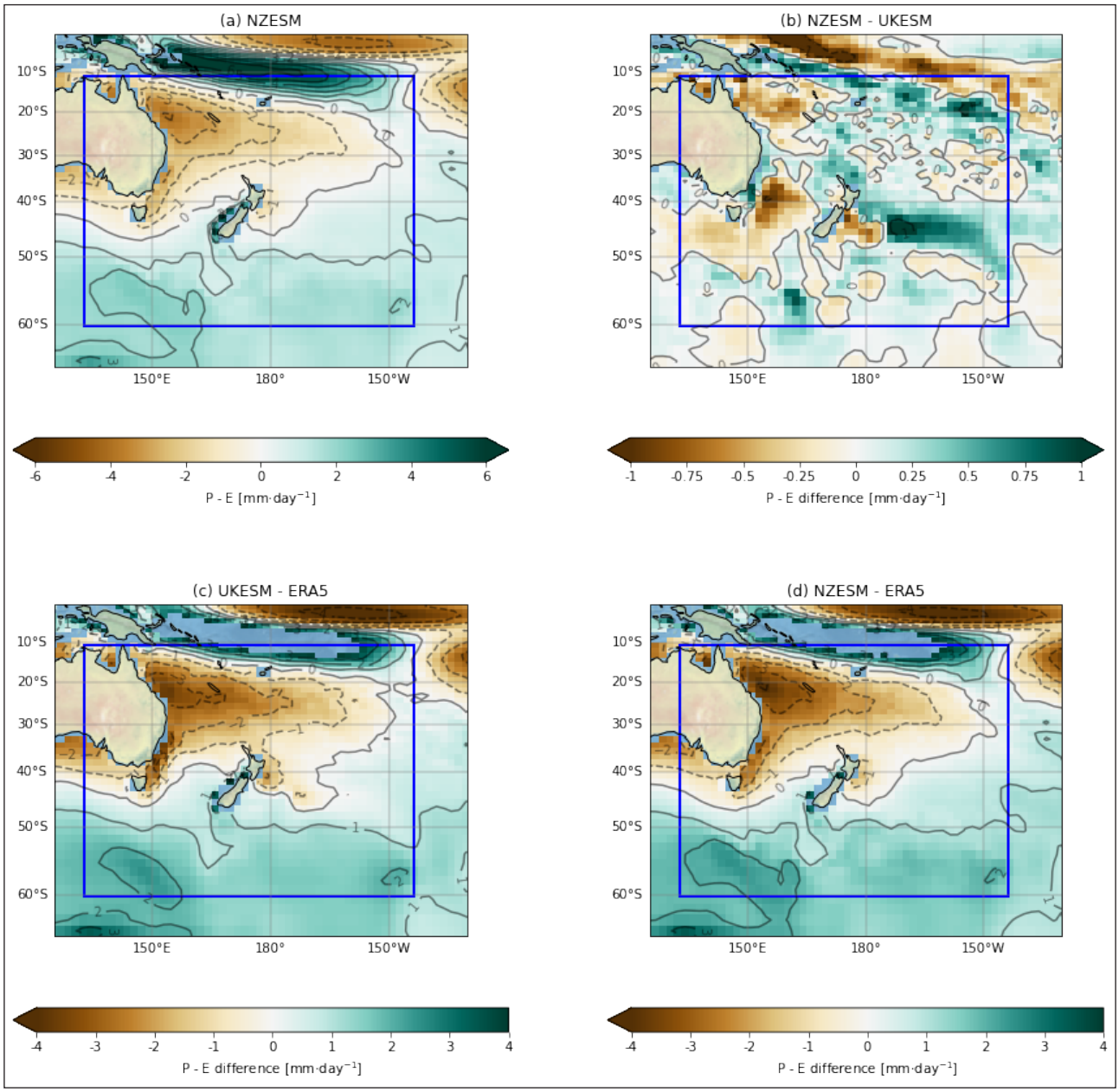

Figure 8: $P - E$ (mm · day^{-1}) for (a) NZESM, (b) NZESM - UKESM, (c) UKESM - ERA5, (d) NZESM ERA5. Contour levels for levels for all plots are at integer values and for (c) and (d) values over 4mm · day^{-1} are masked to aid visual interpretation.

coverage ranges from 0% to 100% and the 15% contour at maximum monthly coverage – September in these models – is often used in the literature as a proxy for maximum extent (Kwok et al, 2009). The yellow lines in Figure 9(b-d) show this contour level for the two models. These intra-model differences notwithstanding, the differences between the models and the observations are an order of magnitude larger, Figure 9(c,d). Therefore the changes made in the NZESM do not make any notable difference to the overall agreement between the models and observations and hence significant model observation disagreement remains.

Due to the warming in the NZESM around -60°, the sea ice retreats southward and allows increased potential evaporation from the ocean surface, thus favouring increased cloud cover. This complex behaviour illustrates the utility of using a coupled climate model to study ocean-ice-atmosphere interactions since in an atmosphere-only climate model configuration, the relationship between sea ice retreat and cloud cover could not be examined at all.

Figure 10 shows the Pearson correlation coefficient between the total cloud amount and the 1.5m temperature for the extra-tropics and is indeed negative everywhere except for some small, isolated patches to the south and east of Australia and a very clear positive signal south of

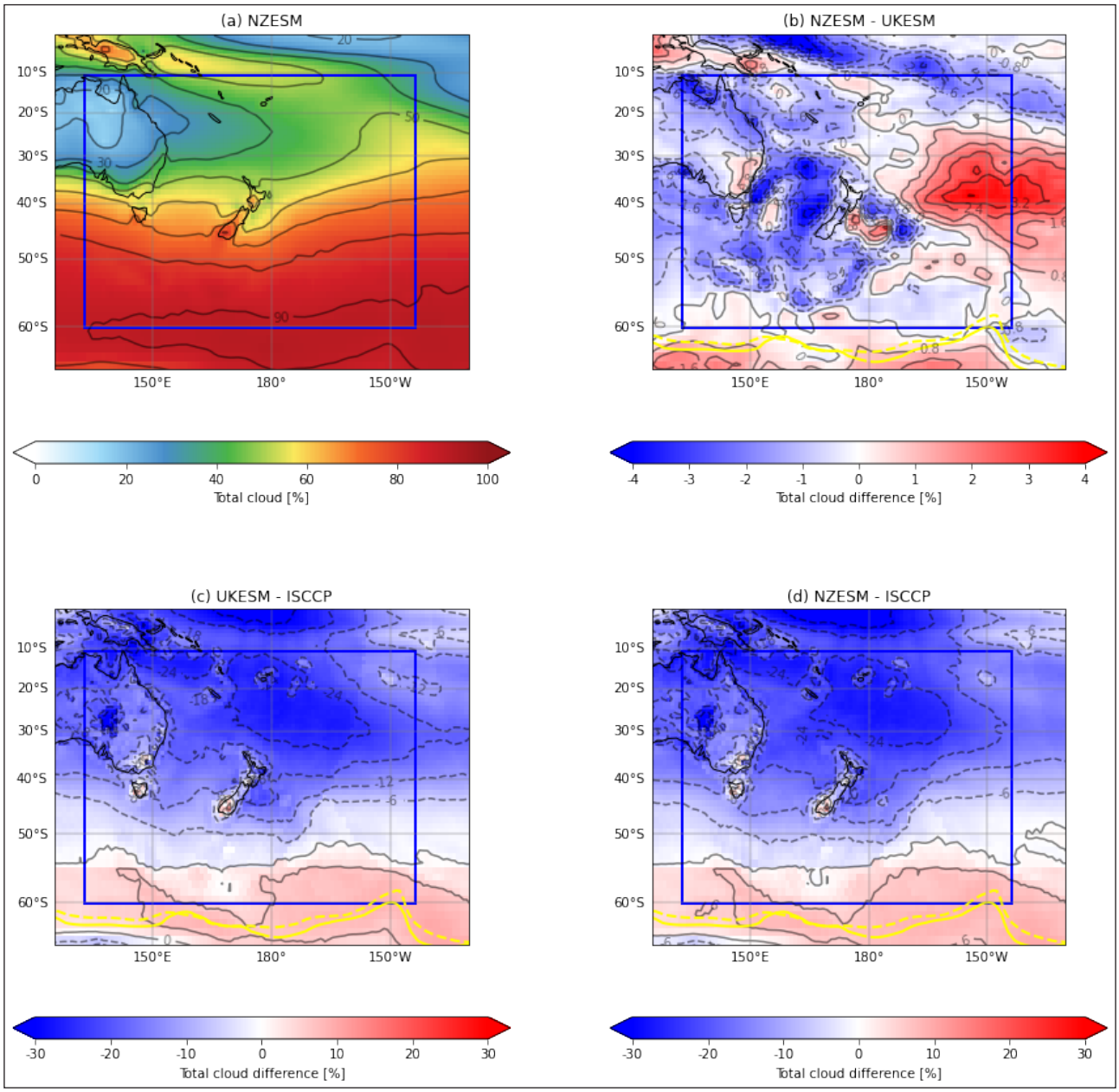

Figure 9: Total cloud for (a) the NZESM, (b) NZESM - UKESM, (c) UKESM - ISCCP, (d) NZESM - ISCCP. Figure (b-d) show 15% grid-box coverage contours of September sea ice cover for UKESM1 (dashed line) and the NZESM (solid line), which is a commonly-used measure of sea ice extent (Kwok et al., 2009) (see main text in S3.2). Observed cloud amount data is from the International Satellite Cloud Climatology Project, ISCCP (Rossow et al., 1999).

the sea ice edge – cf. Figure 9(b-d). Figure 10 is only shown for the extra-tropics to remove the complicating factors of widespread deep convection in the inter-tropical and South Pacific convergence zones.

3.3 Zonal wind and the storm track

3.3.1 Zonal wind

New Zealand's climate is primarily maritime-driven, for example the prevailing westerlies which drive the high rainfall in the South Island's West Coast (Reid et al, 2021). Before examining the position of the storm track, we study the zonal component of the wind. Figure 11 shows this for the same region considered above.

In Figure 11(a) the dominance of the westerlies (i.e. positive u values) is clearly visible and the jet is easily identifiable at around 200hPa and 30°S.

Figure 11(b) shows that there is a small but non-negligible southward shift of the jet in the NZESM and (c), (d) show improvement in model-reanalysis agreement north of ≈ 30°S. This is a further illustration of how improved model physics in one area of a coupled earth system model can have 'downstream' improvements in other

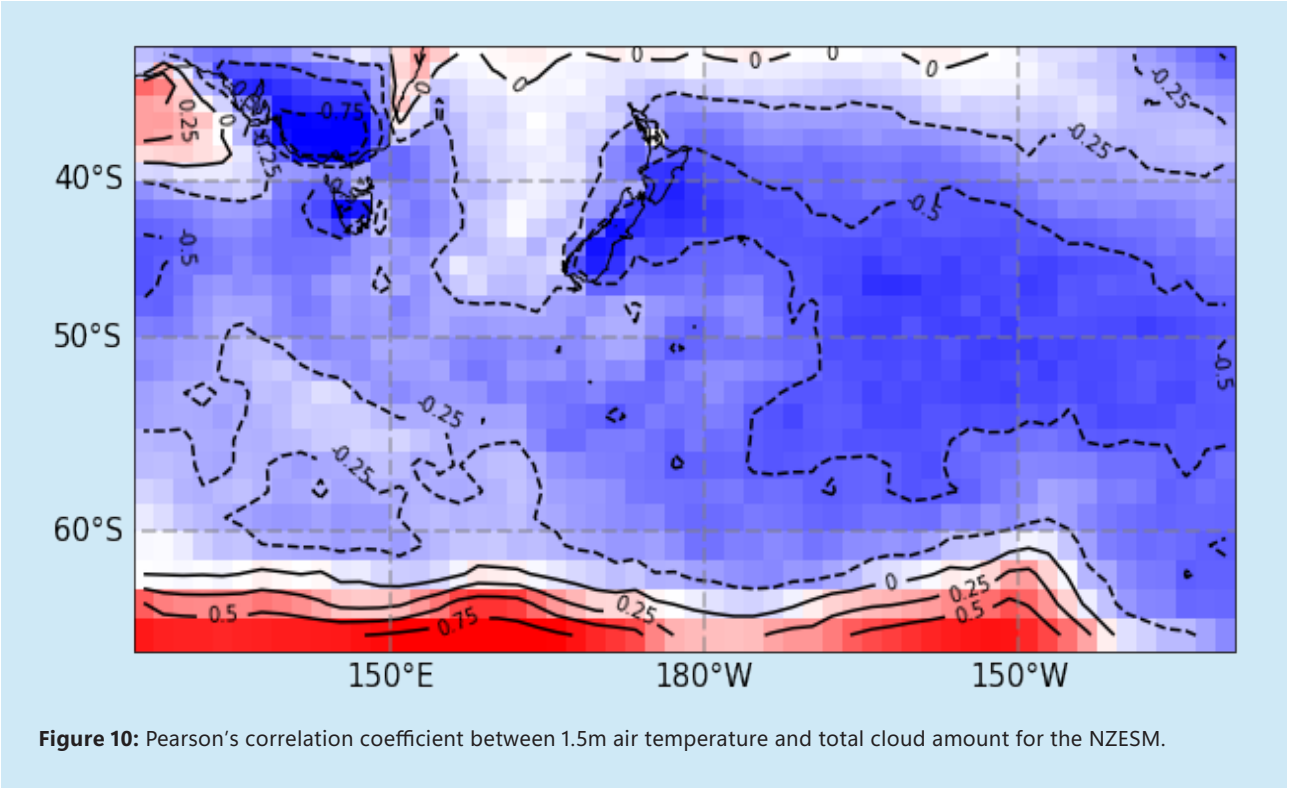

Figure 10: Pearson's correlation coefficient between 1.5m air temperature and total cloud amount for the NZESM.

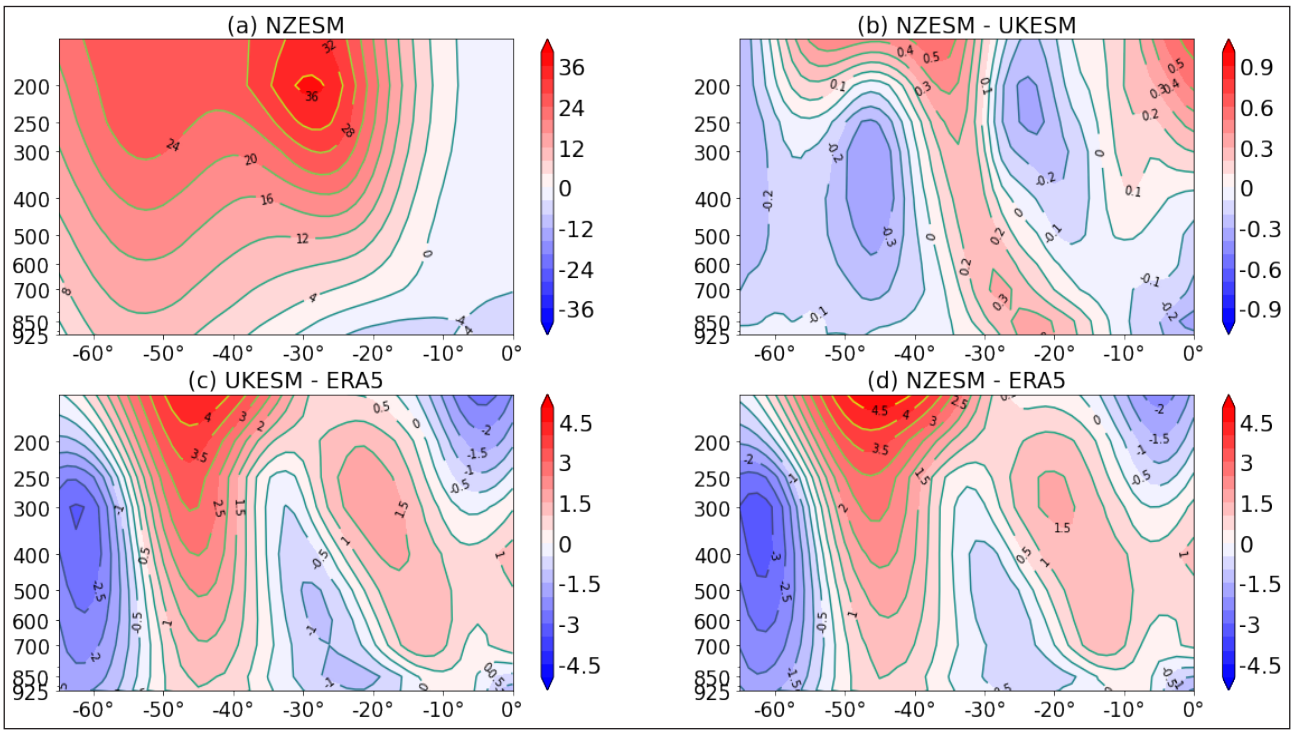

Figure 11: Zonal mean zonal wind (m · s^{-1}) for: (a) NZESM (b) NZESM - UKESM; (c) NZESM - ERA5 reanalysis; (d) UKESM - ERA5 reanalysis.

areas. There is some evidence of model-data deterioration at high southern latitudes which, unsurprisingly, coincides with the decreased fidelity of the air temperature fields considered above.

3.3.2 *Storm track*

Using the stormTracking package (https://github.com/ecjoliver/stormTracking) we have generated maps of the number of unique cyclones – N_c – detected in simulated air pressure data, Figure 12. As its input, this software uses

pressure at mean sea level at six-hourly intervals throughout the 20 year period. The algorithm is split into detection and tracking scripts and is based on a previous study of ocean eddy tracking (Chelton et al, 2011). At each time step, the pressure field is scanned for isolated lows which are then followed through time until they are deemed to have terminated. This Lagrangian-style method allows systems to be followed through time whilst at the same time allowing the number of storms encountered within each grid box to be counted and hence allowing the formation of cyclone density maps, as shown here. An application of this method to tropical cyclones affecting New Zealand can be found elsewhere (Williams et al, 2023) in which a detailed description of the tracking method is included.

Figure 12 shows two main features of the N_c distribution in the NZESM :

1. A general weakening of the storm storm track at latitudes affecting New Zealand, around 30-50°S.
2. Strengthening at higher latitudes, particularly to the north and east of the Ross Sea.

What these changes amount to is a general southerly movement of the storm track and this is particularly evident to the east of New Zealand. Comparing this behaviour with Figure 12(c) shows that there is a general relationship between SST and storm activity; the decrease in SST to the east of New Zealand, for example, is accompanied by a decrease in storm activity. We also see a correspondence south of 60°S where the increase in SST is accompanied by an increase in storm activity.

Although this relationship appears to apply on synoptic scales, it is not universal. For example the NZESM shows an increase in the SST in the immediate vicinity of NZ whilst the storminess shows some evidence of decreasing. This behaviour is somewhat isolated however and may be due to land-sea heat capacity contrast. A more detailed exploration of the models' storm climatologies and how they are predicted to change over the course of the 21st century is the subject of separate work (Williams et al, 2023) and a further study of the midlatitude storm track – addressing for example the relationships between wind, latent heat loss and SST and cloud cover – is currently underway.

4. CONCLUSIONS

In this work we have studied the regional atmospheric climate around New Zealand. We have used historical simulations of the period 1989-2008 using configurations of a coupled earth system model with (Behrens et al, 2020)

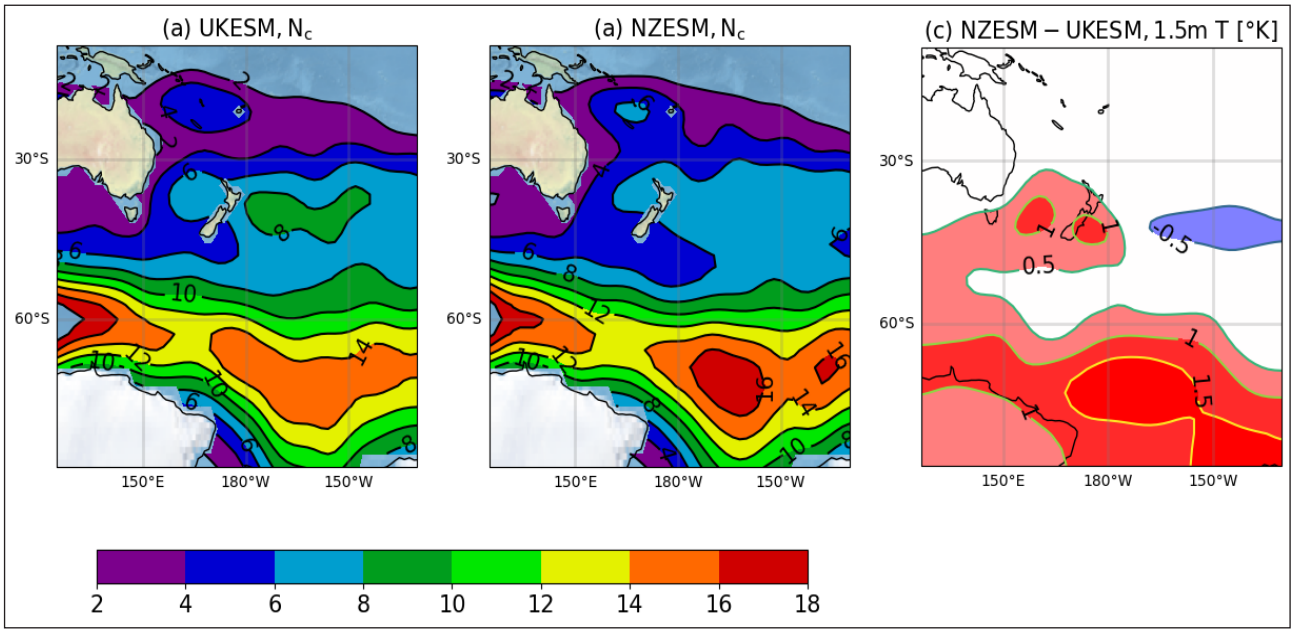

Figure 12: (a) UKESM N_c (b) NZESM N_c (c) NZESM - UKESM 1.5m air temperature difference; all with $\sigma = 2$ in the Gaussian smoothing calculations. The data in (a), (b) is obtained from the stormTracking software and uses the mesoscale feature tracking capability described in (Chelton et al, 2011) by firstly identifying and then following each individual system through time. The number of unique cyclone tracks in each gridbox are then counted in each grid box and smoothed using a Gaussian kernel standard deviation of 2 in the SciPy software (Virtanen et al., 2020). Without this additional smoothing the data are too noisy to enable a reasonable interpretation of the differences between the data sets and since the smoothing reduces the absolute value of N_c the numerical values of the contours are somewhat arbitrary. As a rough guide, the $\sigma = 2$ smoothing reduces the raw N_c values by approximately a factor of 2. The data in (c) is the same as in Figure 1(b) with a southward extension to better illustrate the relationship with the storm track.

and without (Sellar et al, 2019, 2020) a nested, regional ocean model, the introduction of which improves several aspects of model-observation agreement. As is always the case when model physics is altered in the absence of additional model tuning however, the observed changes are not all beneficial. The state-of-theart UKESM1 model was used extensively in the recent 6th Assessment Report of the Intergovernmental Panel on Climate Change and to our knowledge this paper is among the first to consider how a nested ocean model impacts atmospheric climate in a coupled simulation framework.

We have split the analysis into three sections. Firstly we examined the air temperature at the surface and aloft and how this affects surface heat balance. Next, the hydrological response, and finally the effect on the westerly wind structure and the storm track are investigated.

The 1.5m air temperature closely mirrors the improvements seen in the equivalent plots shown in (Behrens et al, 2020). This is of course expected since the data presented are multi-decadal annual means for the same model pair. Above the boundary layer, the NZESM exhibits tropospheric warming and stratospheric cooling, the former of which leads to a general improvement in model-reanalysis agreement and a raising of the tropopause height by an amount comparable to the climate change signal over recent decades. The surface heat balance biases (latent and sensible) are improved in the NZESM cf. UKESM1 with respect to observations and this is particularly striking in the latter.

The SPCZ dominates the precipitation signal and shows a southward shift in the NZESM. The NZESM also shows reduced wet and dry biases close to New Zealand. Evaporation changes are generally of the same sign as the precipitation changes, but larger in magnitude, meaning that $\Delta(P - E)$ is of the opposite sign to ΔP in some areas. The first-order effect of the NZESM's high-resolution ocean is to increase total cloud cover to the east of New Zealand and to decrease it over the Tasman sea and the SPCZ. These cloud changes are generally anticorrelated with surface temperature changes at mid-latitudes, but the reverse is seen at high latitudes near the seasonal sea ice edge. This has been quantified by the inclusion of a map of the correlation coefficient between temperature and cloud cover which makes this assertion explicit.

The structure of the westerly winds shows some improvement in the NZESM and the storm track is shifted south due to the increased eddy-induced warming introduced by the high-resolution ocean. A companion paper on tropical cyclones and their predicted changes through the coming decades is available (Williams et al, 2023) and work to better understand the shift of the mid-latitude storm track is underway. Future work using this nesting methodology on other similarly-related model pairs, as well as this same model pair in different regions would be of significant interest. Additionally, nesting of a high-resolution atmosphere within the global, coupled model would complement the longstanding history of regional atmosphere modelling in New Zealand, e.g. (Ackerley et al, 2012).

APPENDIX

A NZESM computational run-time configuration

Given the significant computational expense of Earth System Models, it is very important to optimise the build and runtime configuration of the component model executables to achieve best efficiency. Ideal setups depend on the characteristics of the target high-performance computing (HPC) platform, such as the number of CPU cores per node, CPU architecture, choice of compilers and libraries, as well as the interconnect that is used for communicating data between the processes that run the model in parallel, and the storage system.

The NZESM consists of separate executables for the atmosphere (Unified Model) and ocean (NEMO) components, which are coupled using the OASIS library (Craig et al, 2017). CPU cores on the HPC need to be distributed between these components to match their respective runtime between data exchanges as closely as possible, as any wait times will reduce efficiency. With the atmosphere model requiring many more cores than the ocean model to handle its much larger computational expense, just enough resources should be assigned to the ocean so that the atmosphere does not need to wait for data to arrive. OASIS comes with a timing feature to help find the right balance.

The Unified Model and NEMO use the Message Passing Library (MPL) for distributed parallel computing, where finding an optimal CPU core count for a given science configuration typically involves trade-offs between runtime and computational efficiency ('strong scaling'). While assigning more cores will speed up computation and thus achieve a higher number of model years per wall clock time interval, communication overheads become more and more important with increasing core count and

reduce computational efficiency, as relatively more time needs to be spent on non-science related computation. It is usually advisable to start with a miminum number of cores that allows the model to meet runtime expectations at reasonable efficiency, especially on a busy HPC, where smaller core counts can lead to shorter queuing times and thus higher overall throughput. If communication overhead is still small and if there is enough capacity on the HPC, core counts can be increased to reduce runtime without suffering much efficiency loss ('linear scaling').

Both the Unified Model and NEMO impose constraints on how CPU cores can be used for parallel computing with the 'domain decomposition' approach, which can prevent configurations from using all available cores on the assigned HPC nodes and thus impact efficient resource utilisation.

The Māui HPC that was used for this work comes with 40 Intel Skylake CPU cores per node. The original core count configuration of NZESM was readjusted for Maui to minimise atmosphere/ocean runtime imbalance, minimise the number of unused cores on the nodes, and maximise MPI parallelisation efficiency. This led to a 28% node count reduction from 32 nodes to 23 with only a modest 5% increase in runtime from 7.7 hours per model year to 8.1 hours per model year. Overall computational resource utilisation by the NZESM was thus reduced by 24%.

ACKNOWLEDGEMENTS

This paper obtained funding and support through the Ministry of Business Innovation and Employment Deep South National Science Challenge projects (C01X1412) and Royal Society Marsden Fund (NIW1701). The development of UKESM1, was supported by the Met Office Hadley Centre Climate Programme funded by BEIS and Defra (GA01101) and by the Natural Environment Research Council(NERC) national capability grant for the UK Earth System Modelling project, grant number NE/N017951/1. The authors would also like to acknowledge the support and collaboration of the wider Unified Model Partnership, https://www.metoffice.gov.uk/research/approach/collaboration/unified-model/partnership and the use of New Zealand eScience Infrastructure (NeSI) high performance computing facilities, consulting support and training services as part of this research. New Zealand's national facilities are provided by NeSI and funded jointly by NeSI's collaborator institutions and through the Ministry of Business, Innovation & Employment's Research Infrastructure programme, www.nesi.org.nz. The ocean and sea ice code used in this work is available online at https://doi.org/10.5281/zenodo.3873691.

REFERENCES

Ackerley, D. et al. (2012). Regional climate modelling in New Zealand: Comparison to gridded and satellite observations. In: *Weather and Climate* 32.1, pp. 3–22. http://www.jstor.org/ stable/26169722.

Archibald, A. T. et al. (2020). Description and evaluation of the UKCA stratosphere–troposphere chemistry scheme (StratTrop vn 1.0) implemented in UKESM1. In: *Geoscientific Model Development* 13.3, pp. 1223–1266.

Beadling, R. L. et al. (2020). Representation of Southern Ocean Properties across Coupled Model Intercomparison Project Generations: CMIP3 to CMIP6. In: *Journal of Climate* 33.15, pp. 6555–6581. https://doi.org/10.1175/JCLI-D-19-0970.1.

Behrens, Erik (2013). The oceanic response to Greenland melting: the effect of increasing model resolution. en. PhD thesis.

Behrens, Erik (2020). erikbehrens/NZESM1: *First release of the NZESM* (ocean+sea ice code). Version v1.0. https://doi.org/10.5281/zenodo.3873691.

Behrens, Erik et al. (2012). Model simulations on the long-term dispersal of 137Cs released into the Pacific Ocean off Fukushima. In: *Environmental Research Letters* 7.3, p. 034004.

Behrens, Erik et al. (2020). Local Grid Refinement in New Zealand's Earth System Model: Tasman Sea Ocean Circulation Improvements and Super-Gyre Circulation Implications. In: *Journal of Advances in Modeling Earth Systems* 12.7. https://doi.org/10.1029/2019MS001996.

Behrens, Erik et al. (2022). Projections of future marine heatwaves for the oceans around New Zealand using New Zealand's earth system model. In: *Frontiers in Climate* 4, p. 798287.

Biastoch, Arne et al. (2008). Agulhas leakage dynamics affects decadal variability in Atlantic overturning circulation. In: *Nature* 456.7221, pp. 489–492.

Bodas-Salcedo, Alejandro et al. (2011). COSP: Satellite simulation software for model assessment. In: *Bulletin of the American Meteorological Society* 92.8, pp. 1023–1043.

Brown, AR et al. (2008). Upgrades to the boundary-layer scheme in the Met Office numerical weather prediction model. In: *Boundary-Layer Meteorology* 128.1, pp. 117–132.

Chelton, Dudley B. et al. (2011). Global observations of nonlinear mesoscale eddies. In: *Progress in Oceanography* 91.2, pp. 167–216. https://doi.org/10.1016/j.pocean.2011.01.002.

Craig, Anthony et al. (2017). Development and performance of a new version of the OASIS coupler, OASIS3-MCT_3.0. In: *Geoscientific Model Development* 10.9, pp. 3297–3308.

Debreu, Laurent et al. (2008). AGRIF: Adaptive grid refinement in Fortran. In: *Computers & Geosciences* 34.1, pp. 8–13.

Edwards, J. M. et al. (1996). Studies with a flexible new radiation code. I: Choosing a configuration for a large-scale model. In: *Quarterly Journal of the Royal Meteorological Society* 122.531, pp. 689–719. https://doi.org/10.1002/qj.49712253107.

Good, Simon A et al. (2013). EN4: Quality controlled ocean temperature and salinity profiles and monthly objective analyses with uncertainty estimates. In: *Journal of Geophysical Research: Oceans* 118.12, pp. 6704– 6716.

Gregory, D. et al. (1990). A Mass Flux Convection Scheme with Representation of Cloud Ensemble Characteristics and Stability-Dependent Closure. In: *Monthly Weather Review* 118.7, pp. 1483–1506.

Gurvan, Madec et al. (2022). *NEMO ocean engine*. Version v4.2. https://doi.org/10.5281/zenodo.6334656.

Hawcroft, Matt et al. (2016). Southern Ocean albedo, inter-hemispheric energy transports and the double ITCZ: global impacts of biases in a coupled model. In: *Climate Dynamics* 48.7-8, pp. 2279–2295.

Hersbach, Hans et al. (2020). The ERA5 global reanalysis. In: *Quarterly Journal of the Royal Meteorological Society* 146.730, pp. 1999–2049.

Hewitt, Helene T et al. (2020). Resolving and parameterising the ocean mesoscale in earth system models. In: *Current Climate Change Reports* 6, pp. 137–152.

Hoem, Frida S. et al. (2022). Strength and variability of the Oligocene Southern Ocean surface temperature gradient. In: *Communications Earth & Environment* 3.1, p. 322.

Hourdin, Frédéric et al. (2017). The Art and Science of Climate Model Tuning. In: *Bulletin of the American Meteorological Society* 98.3, pp. 589–602.

Hunke, Elizabeth et al. (2017). CICE, *The Los Alamos Sea Ice Model*, Version 00.

Hyder, Patrick et al. (2018). Critical Southern Ocean climate model biases traced to atmospheric model cloud errors. In: *Nature Communications* 9.1. DOI: 10.1038/s41467-018-05634-2.

Kwok, R. et al. (2009). Decline in Arctic sea ice thickness from submarine and ICESat records: 1958–2008. In: *Geophysical Research Letters* 36.15. DOI: https://doi.org/10.1029/2009GL039035.

Luo, Fengyun et al. (2023). Origins of Southern Ocean warm sea surface temperature bias in CMIP6 models. In: *npj Climate and Atmospheric Science* 6.1, p. 127.

McNeall, Doug et al. (2020). Correcting a bias in a climate model with an augmented emulator. In: *Geoscientific Model Development* 13.5, pp. 2487–2509.

Meng, Lingyunetal. (2021). Continuous rise of the tropopause in the Northern Hemisphere over 1980 & 2013; 2020. In: *Science Advances* 7.45, eabi8065.

Pisoft, Petr et al. (2021). Stratospheric contraction caused by increasing greenhouse gases. In: *Environmental Research Letters* 16.6, p. 064038.

Reid, Kimberley J. et al. (2021). Extreme rainfall in New Zealand and its association with Atmospheric Rivers. In: *Environmental Research Letters* 16.4, p. 044012.

Ridley, Jeff K. et al. (2018). The sea ice model component of HadGEM3-GC3. 1. In: *Geoscientific Model Development* 11.2, pp. 713–723.

Rossow, W. B. et al. (2004). The international satellite cloud climatology project (ISCCP) website: An online resource for research. In: *Bulletin of the American Meteorological Society* 85.2, pp. 167–172.

Rossow et al. (1999). Advances in understanding clouds from ISCCP. In: *Bulletin of the American Meteorological Society* 80.11, pp. 2261–2288.

Schmidt, Gavin A. et al. (2017). Practice and philosophy of climate model tuning across six US modeling centers. In: *Geoscientific Model Development* 10.9, pp. 3207–3223.

Schwarzkopf, F. U. et al. (2019). The INALT family – a set of high-resolution nests for the Agulhas Current system within global NEMO ocean/sea-ice configurations. In: *Geoscientific Model Development* 12.7, pp. 3329–3355.

Sellar, Alistair A. et al. (2019). UKESM1: Description and evaluation of the UK Earth System Model. In: *Journal of Advances in Modeling Earth Systems* 11.12, pp. 4513–4558.

Sellar, Alistair A. et al. (2020). Implementation of U.K. Earth System Models for CMIP6. In: *Journal of Advances in Modeling Earth Systems* 12.4. https://doi.org/10.1029/2019MS001946.

Tang, Yongming et al. (2019). MOHC UKESM1.0-LL model output prepared for CMIP6 CMIP historical. DOI: 10.22033/ESGF/CMIP6.6113.

Taylor, Karl E. et al. (2012). An overview of CMIP5 and the experiment design. In: *Bulletin of the American Meteorological Society* 93.4, pp. 485–498.

Varma, Vidya et al. (2020). Improving the Southern Ocean cloud albedo biases in a general circulation model. In: *Atmospheric Chemistry and Physics* 20.13, pp. 7741–7751.

Virtanen, Pauli et al. (2020). SciPy 1.0: Fundamental Algorithms for Scientific Computing in Python" In: *Nature Methods* 17, pp. 261–272.

Walters, David et al. (2019). The Met Office Unified Model global atmosphere 7.0/7.1 and JULES global land 7.0 configurations. In: *Geoscientific Model Development* 12.5, pp. 1909–1963.

Williams, Jonny et al. (2016). Development of the New Zealand Earth System Model: NZESM. In: *Weather and Climate* 36, pp. 25–44. https://www.jstor.org/stable/26779386.

Williams, Jonny et al. (2023). Coupled atmosphere-ocean simulations of contemporary and future South Pacific tropical cyclones. In: *EGUsphere* 2023, pp. 1–31.

Wood, Nigel et al. (2014). An inherently mass-conserving semi-implicit semi-Lagrangian discretization of the deep-atmosphere global non-hydrostatic equations. In: *Quarterly Journal of the Royal Meteorological Society* 140.682, pp. 1505–1520. https://doi.org/10.1002/qj.2235.

Yool, A. et al. (2013). MEDUSA-2.0: an intermediate complexity biogeochemical model of the marine carbon cycle for climate change and ocean acidification studies. In: *Geoscientific Model Development* 6.5, pp. 1767–1811.

Yool, A. et al. (2021). Evaluating the physical and biogeochemical state of the global ocean component of UKESM1 in CMIP6 historical simulations. In: Geoscientific Model Development 14.6, pp. 3437–3472.

Yu, Lisanetal. (2007). Objectively Analyzed Air–Sea Heat Fluxes for the Global Ice-Free Oceans (1981–2005). In: *Bulletin of the American Meteorological Society* 88.4, pp. 527–540.